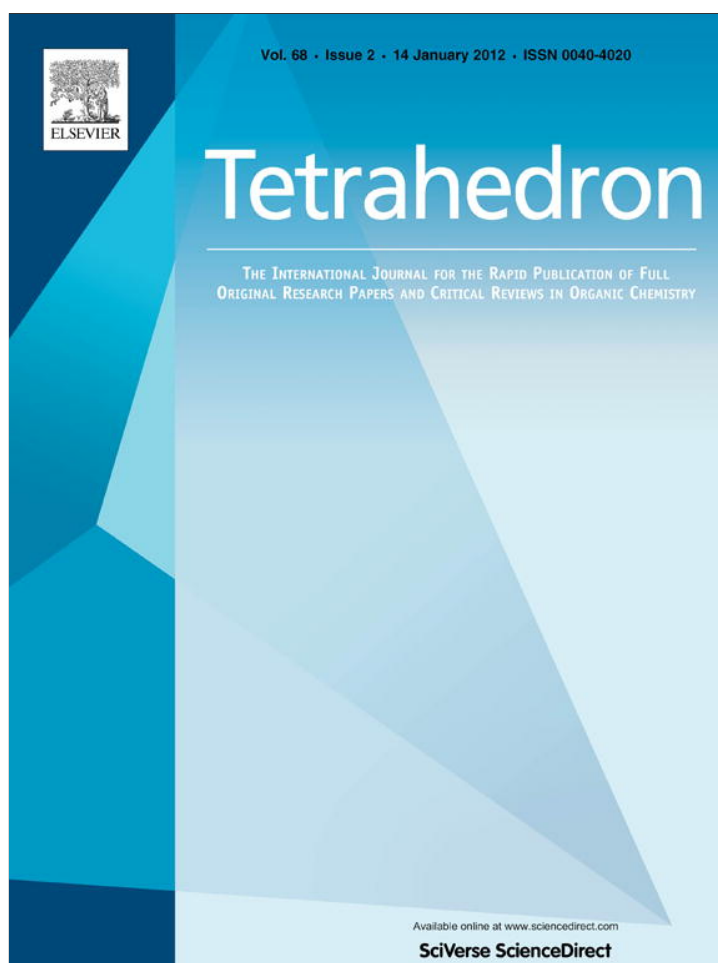


Provided for non-commercial research and education use.
Not for reproduction, distribution or commercial use.



This article appeared in a journal published by Elsevier. The attached copy is furnished to the author for internal non-commercial research and education use, including for instruction at the authors institution and sharing with colleagues.

Other uses, including reproduction and distribution, or selling or licensing copies, or posting to personal, institutional or third party websites are prohibited.

In most cases authors are permitted to post their version of the article (e.g. in Word or Tex form) to their personal website or institutional repository. Authors requiring further information regarding Elsevier's archiving and manuscript policies are encouraged to visit:

<http://www.elsevier.com/copyright>



Contents lists available at SciVerse ScienceDirect

Tetrahedron

journal homepage: www.elsevier.com/locate/tet

Theoretical and experimental study on the reactivity of methyl dichlorobenzoates with sulfur-centered nucleophiles by electron transfer reactions

Jorge G. Uranga, Juan P. Montañez, Ana N. Santiago*

INFIQC, Departamento de Química Orgánica, Facultad de Ciencias Químicas, Universidad Nacional de Córdoba, Ciudad Universitaria, Córdoba 5000, Argentina

ARTICLE INFO

Article history:

Received 2 September 2011

Received in revised form 28 October 2011

Accepted 31 October 2011

Available online 6 November 2011

Keywords:

Electron transfer

Herbicide

Thiolate group

DFT

ABSTRACT

Reactions of methyl 2,5-dichlorobenzoate or methyl 3,6-dichloro-2-methoxybenzoate with sulfur-centered nucleophiles gave mono- and disubstitution products, respectively through $S_{RN}1$ mechanism in liquid ammonia. Products obtained could be potential herbicides less toxic to the environment. Theoretical studies explained the reactivity observed considering geometries, and spin densities of radical anions and potential energy surfaces for the dissociation of the radical anions formed.

© 2011 Elsevier Ltd. All rights reserved.

1. Introduction

3,6-Dichloro-2-methoxybenzoic acid (Dicamba[®]) or methyl 3,6-dichloro-2-methoxybenzoate (Disugran[®]) have been widely used as herbicides in different countries. Dicamba[®] is a chlorinated synthetic auxin analog, relatively stable under natural conditions, which has become a prominent pollutant for soils and aquatic systems. In order to produce new, environmentally friendly, herbicides, we decided to investigate the reaction of Disugran[®] and methyl 2,5-dichlorobenzoate with sulfur-centered nucleophiles.

It is well known that aryl iodides (ArI), bromides (ArBr), and ArN_2F_4B can afford substitution products with different aryl thiolates with good yields by the Unimolecular Radical Nucleophilic Substitution ($S_{RN}1$) mechanism.¹ For instance, ArI reacts with phenylthiolate (PhS^-),² substituted ArS^- ,³ 2-naphthalene thiolate,⁴ and heteroarene thiolate⁵ ions when they are photostimulated in liquid ammonia, affording good yields of substitution products. Depending on the experimental conditions, a competition between $S_{RN}1$ and S_NAr mechanisms has been proposed for the reaction of ArX with PhS^- ions.⁶ Furthermore, dihalobenzenes and $BrArN_2F_4B$ afford disubstitution products in most cases.⁷

Alkyl thiolates (RS^-) can also react with ArX by $S_{RN}1$. In these cases, the fragmentation of the intermediate radical anion ($ArSR^-$) at the $S-C_{alkyl}$ bond leads to the formation of $ArSH$ (scrambling

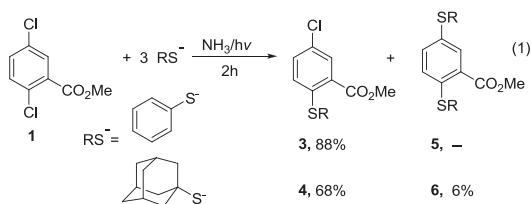
product), particularly with unactivated $ArCl$.¹ For instance, $p-C_6H_4Cl_2$ reacts with $n-BuS^-$ affording $p-HSC_6H_4-SBu-n$ (94% yield), involving both substitution and fragmentation processes.⁸ However, the photostimulated reaction of 1-iodoadamantane (IAd) with PhS^- in liquid ammonia affords a single substitution product (45% yield), demonstrating that $(PhSAd)^-$ does not fragment under these conditions.⁹ Saveant et al. have exclusively reported substitution products during the photostimulated reaction of IAd with diverse ArS^- derivatives in acetonitrile.¹⁰

The main goal of this study was to carry out the synthesis of new, effective but less toxic auxin derivatives. Thus, we tested the reactivity of methyl 2,5-dichlorobenzoate (**1**) and methyl 3,6-dichloro-2-methoxybenzoate (**2**) with sulfur-centered nucleophiles [PhS^- and 1-adamantylthiolate (AdS^-)] by the $S_{RN}1$ mechanism. Additionally, theoretical calculations were performed to fully understand the reactivity of methyl dichlorobenzoates derivatives.

2. Results and discussion

The photostimulated reaction of PhS^- or AdS^- ions with **1** afforded good yields of the monosubstitution product with retention of chlorine (**3** or **4**) using liquid ammonia as the solvent (Eq. 1). These reactions were stimulated by light and inhibited by $S_{RN}1$ inhibitors (Table 1 expts 1–3 or 5–7). In DMSO, the photostimulated reaction of **1** with these anions afforded mainly the hydrolysis of substrates, demonstrating that hydrolysis competes efficiently with substitution in this solvent.

* Corresponding author. Tel./fax: +54 351 4334170; e-mail address: santiago@fcq.unc.edu.ar (A.N. Santiago).

**Table 1**

Reactions of methyl 2,5-dichlorobenzoate or methyl 3,6-dichloro-2-methoxybenzoate with phenylthiolate or adamantylthiolate during 120 min

	Substrate (10 ⁻³ M) ^a	Nucleophile (10 ⁻² M)	Condition	Cl ⁻ b (%)	Yield of substitution ^c	
					mono-	di-
1	1 (3.8)	PhS ⁻ (1.2)	NH ₃ , hν	77	3 , 88	—
2	1 (4.0) ^d	PhS ⁻ (1.2)	NH ₃ , dark	<3	—	—
3	1 (4.1)	PhS ⁻ (1.2)	NH ₃ , hν ^e	<3	—	—
4	1 (3.8)	PhS ⁻ (1.9)	NH ₃ , hν	65	3 , 67	5 , —
5 ^f	1 (4.0)	AdS ⁻ (1.2)	NH ₃ , hν	72	4 , 68	6 , 6
6 ^f	1 (4.0)	AdS ⁻ (1.2)	NH ₃ , dark	<3	—	—
7 ^f	1 (4.0)	AdS ⁻ (1.2)	NH ₃ , hν ^e	<3	—	—
8 ^f	1 (4.0)	AdS ⁻ (2.0)	NH ₃ , hν	114	4 , 62	6 , 22
9	2 (3.7)	PhS ⁻ (1.2)	NH ₃ , hν	78	—	9 , 80
10	2 (3.8)	PhS ⁻ (1.2)	NH ₃ , dark	<3	—	—
11	2 (3.7)	PhS ⁻ (1.2)	NH ₃ , hν ^e	<3	—	—
12	2 (4.1)	PhS ⁻ (0.4)	NH ₃ , hν	40	—	9 , 44
13 ^f	2 (4.1)	AdS ⁻ (1.2)	NH ₃ , hν	nq	—	10 , 98
14 ^f	2 (3.8)	AdS ⁻ (1.2)	NH ₃ , dark	<3	—	—
15 ^f	2 (3.8)	AdS ⁻ (1.2)	NH ₃ , hν ^e	<3	—	—
16 ^f	2 (4.0)	AdS ⁻ (0.4)	NH ₃ , hν	42	—	10 , 52
17 ^g	2 (0.92)	AdS ⁻ (0.25), PhS ⁻ (0.25)	NH ₃ , hν	nq	—	9 , 48 14 , 38 ^h 10 , 9
18	15 (1.4)	PhS ⁻ (8.6)	NH ₃ , hν	<3	—	—
19	16 (1.4)	PhS ⁻ (8.6)	NH ₃ , hν	82	17 , 74	—

^a Nonreactive substrates recovered as acids in all the reactions.

^b Chloride ions determined by potentiometry.

^c Organic products, after acidification with HNO₃ to pH ≈ 3, were determined by GC using internal standards.

^d This substrate was recovered as amide.

^e With 30% *m*-DNB added.

^f Reactions quenched with Mel.

^g Ref. 14.

^h Relative areas 1:1.

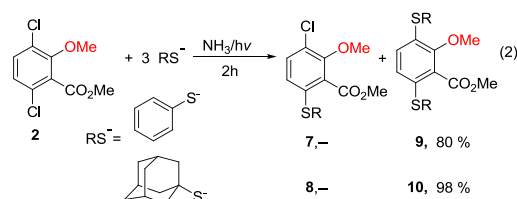
It is not surprising that *ortho*-substitution with respect to the ester group was the preferred position during these reactions. Similar results were found during the dark reaction of **1** with Me₃Sn⁻ ions, with methyl 5-chloro-2-(trimethylstannyl)benzoate (*ortho*-substitution) as the main product with 81% yield.¹¹ This reactivity has been explained by theoretical calculations, showing potential energy surfaces of **1** for two possible fragmentations, evidencing that the *ortho* fragmentation has substantially lower activation energy than the corresponding to the *meta*-position.¹²

In order to obtain disubstitution products (**5** or **6**), we decided to carry out these reactions increasing the nucleophile concentration. Under these conditions, **1** reacted with PhS⁻ affording only **3**, and **5** was not detected (Table 1 expt 4).

However, **1** reacted with AdS⁻ affording the monosubstitution product with retention of chlorine (62%) and low yield (22%) of the disubstitution product **6** (Table 1 expt 8). Theoretical calculations discussed below were helpful in explaining these results, i.e., the exclusive formation of the monosubstitution products and the presence of minor amounts of the disubstitution product as well (see Computational analysis).

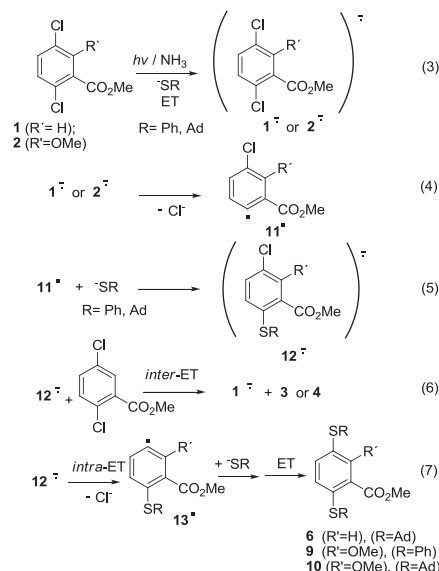
On the other hand, methyl 3,6-dichloro-2-methoxybenzoate (**2**) reacted with either PhS⁻ or AdS⁻ affording only disubstitution products (**9** or **10**) in good yields using liquid ammonia as the solvent (Eq. 2). These reactions were also stimulated by light and

inhibited by *m*-dinitrobenzene (*m*-DNB, S_{RN}1 inhibitor) (Table 1 expts 9–11 or 13–15).



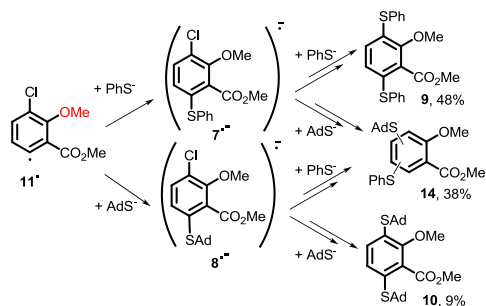
In order to evaluate the formation of monosubstitution products, we carried out reactions shown in Eq. 2, using a deficit of the nucleophile (nucleophile/substrate ratio=1:1). Such monosubstitution product (**7** or **8**) was not formed (expts 12 and 16, Table 1). Furthermore, methyl iodide was added to quench anions showing that no scrambling products were formed during reactions with AdS⁻, which confirms that the intermediate radical anions (ArSAd)^{-•} are not fragmented at the S–C_{alkyl} bond.

Considering that these reactions were stimulated by light, the formation of substitution products and inhibition in the presence of *m*-DNB suggests that these reactions occur by the S_{RN}1 mechanism, as shown in Scheme 1. When **1** or **2** receives one electron, its radical anion **1^{•-}** or **2^{•-}** is formed (Eq. 3). This radical anion affords radical **11[•]** by fragmentation of the C–Cl bond (Eq. 4), giving a new radical anion **12^{•-}** by reaction with the nucleophile (Eq. 5). This radical anion **12^{•-}** affords the monosubstitution product **3** or **4** by intermolecular electron transfer (*inter*-ET) to the substrate (Eq. 6), or forms radical **13[•]** by intramolecular ET step (*intra*-ET) to the second C–Cl bond (Eq. 7). In this case, radical **13[•]** affords the radical anion corresponding to the disubstitution product by coupling with the nucleophile, which by an ET reaction, yields disubstitution product, **6**, **9** or **10** (Eq. 7).

**Scheme 1.**

As can be seen, radical anion **12^{•-}** has two competitive reactions: an *inter*-ET to the substrate or an *intra*-ET to the second C–Cl bond. The later reaction was observed with compound **2**, while the first one dominated with compound **1**.

In an attempt to explain the diverse reactivity of both nucleophiles used in this work, we evaluated their relative reactivity by competition experiments. In these experiments, the reactivity depends on the rates of the coupling reaction between the radical intermediate **11**• and the nucleophiles studied.¹³ The photostimulated reaction of an excess of PhS⁻ and AdS⁻ with **2** afforded disubstitution products (**9**, **10** and **14**) using liquid ammonia (Scheme 2). Product **14** was obtained as an equimolecular mixture of two isomers. These competition reactions¹⁴ demonstrated that the relative reactivity of the photostimulated reaction between PhS⁻ and **2** was 2.4 times higher than that corresponding to AdS⁻ (Table 1, expt 17).



Scheme 2.

Theoretical calculations also helped to understand the difference in reactivity found for these nucleophiles, although steric effects can be clearly attributed as a probable cause.

In order to understand different reactivity between **7**•⁻ and **8**•⁻, we carried out the reaction of PhS⁻ with methyl 3-chloro-2-methoxybenzoate (**15**) or methyl 6-chloro-2-methoxybenzoate (**16**). The *meta*-chloro derivative (**15**) did not react, while the *ortho*-chloro derivative (**16**) afforded 74% yields of the substitution product, methyl 2-methoxy-6-(phenylthio)benzoate (**17**) under irradiation (Table 1 expts 18 and 19). These results suggest that **15**•⁻ was formed but does not fragment under these conditions, which is well explained by computational studies.

2.1. Computational analysis

To further understand our current experimental results, we carried out DFT based calculations with Gaussian 03.¹⁵ Optimized structures for compounds **1**•⁻ and **2**•⁻ showed an in-plane distortion from the optimal sp² Cl_{ortho}-C_{ipso}-C₁ angle (120°), which are 122.5° and 124.2°, respectively. It has been reported that a distortion from the optimal sp² could facilitate the fragmentation of radical anions¹⁶ as well as the spin distribution can also be used to predict the dissociation observed for radical anions intermediates.¹⁷ Fig. 1 shows the spin density of radical anions **1**•⁻, **2**•⁻, **15**•⁻, and **16**•⁻. It is clear that the spin density of these compounds is significant in its *ortho*-position with respect to the ester group, whereas it is almost zero at its *meta*-positions. These spin density distributions indicate that the cleavage of radical anions could be facilitated with chlorides bonded at the *ortho*-position. These results are consistent with our experiments and therefore we propose the formation of radical **11**• as intermediate in these reactions.

The geometries and spin density of substituted radical anions **3**•⁻, **4**•⁻, **7**•⁻, and **8**•⁻ are shown in Fig. 2, while thermodynamic and kinetic parameters of the anionic potential energy surface are presented in Table 2. The spin distributions for **3**•⁻ and **4**•⁻ are similar to that of **1**•⁻, with an almost zero spin density at its *meta*-positions with respect to the ester group. These spin density distributions explain why the cleavages of radical anions are not facilitated at the *meta*-position. Under these conditions, the formation of monosubstitution product with retention of chloro,

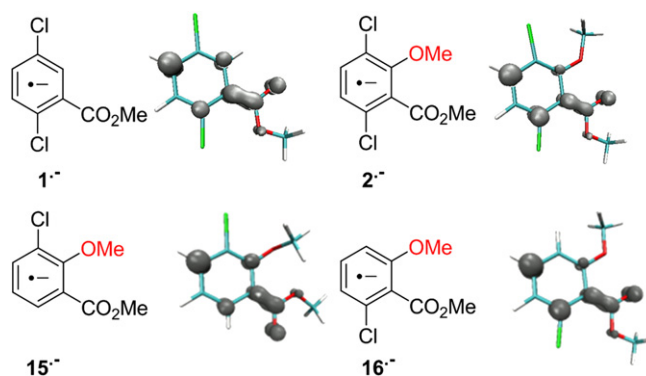
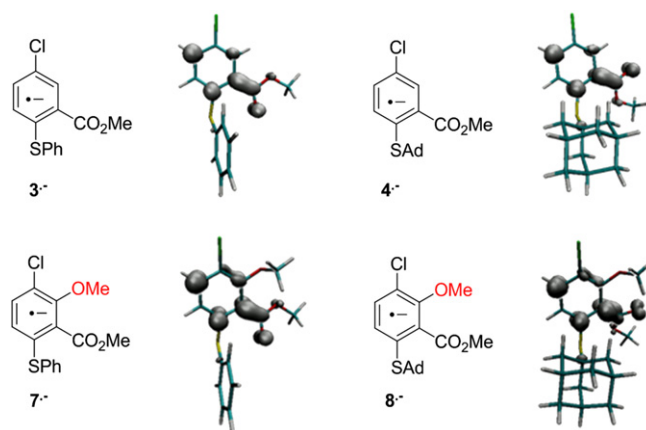
Fig. 1. Geometry and unpaired spin distribution of radical anions **1**•⁻, **2**•⁻, **15**•⁻, and **16**•⁻.Fig. 2. Geometry and unpaired spin distribution of radical anions **3**•⁻, **4**•⁻, **7**•⁻, and **8**•⁻.

Table 2

Main geometric, thermodynamic, and kinetic parameters of the anionic surface for the dissociation of radical anions in gas phase

Compounds ^a		3 • ⁻	4 • ⁻	7 • ⁻	8 • ⁻	15 • ⁻
-EA ^b		-20.56	-16.45	-13.09	-9.98	-11.97
AE ^c		10.90	9.95	5.83	4.26	8.78
Radical anion	C _{ipso} -Cl ^d	1.79	1.79	1.78	1.78	1.78
	α ^e	1.3	1.5	4.5	7.1	0.4
	β ^f	0.5	4.4	17.5	28.2	0.9
Transition state	C _{ipso} -Cl ^d	2.11	2.08	1.93	1.89	2.11
	α ^e	34.9	33.1	31.4	29.9	35.4
	β ^f	32.4	37.4	61.5	57.9	12.8

^a B3LYP/6-31+G*/6-31+G* values ZPE corrected in kcal/mol.

^b EA=Adiabatic Electron affinity (RX→RX⁻).

^c AE=Activation Energy.

^d Distance C_{ipso}-Cl in Å.

^e Dihedral angle α Cl-C_{ipso}-C₂-C₄ in degrees, where C₂ and C₄ are neighbor to C_{ipso} (shows C_{ipso}-Cl deviation out of plane).

^f Dihedral angle β O_{C=O}-C_{C=O}-C₁-C₆ in degrees (shows CO₂Me group deviation in plane).

such as **3** or **4** is expected, in complete agreement with our current experimental results.

In contrast, compounds **7**•⁻ and **8**•⁻ show that the ester group is rotated out of the ring plane (Table 2, Dihedral angle β O_{C=O}-C_{C=O}-C_{ipso}-C₆), presumably as a consequence of steric repulsions on the more crowded ring, which decreases the contribution of the ester group in the overall spin distribution. Therefore, the spin distribution for **7**•⁻ or **8**•⁻, show spin contributions at its *meta*-position, facilitating the *intra*-ET to the second Cl-C_{ipso} bond.

The rotated ester group in $7^{\cdot-}$ and $8^{\cdot-}$ also decreases the stability of radical anions, owing to the loss of conjugation between the aryl ring and the ester group, showing lower electron binding energies in these radical anions ($-EA$, Table 2). The methoxy (electron donating) group also decreases the stability of these radical anions.¹⁸

According to our calculations, the radical anion $15^{\cdot-}$ is produced easier than $16^{\cdot-}$. This is so because the compound **15** has less electron affinity than **16** (-11.97 and -8.24 kcal/mol, respectively). However, only compound **16** afforded substitution product, which indicates that both radical anions are formed, but only $16^{\cdot-}$ fragments. The radical anion $15^{\cdot-}$ shows the ester group in the ring plane and an almost zero spin density at its *meta*-positions, avoiding the cleavage of the radical anion at the *meta*-position.

The gas phase potential energy surfaces (PES), evaluated for the dissociation of radical anions $3^{\cdot-}$, $4^{\cdot-}$, $7^{\cdot-}$, and $8^{\cdot-}$, are presented in the Fig. 3. As observed in Fig. 3 and Table 2, radical anions arising from **2** ($7^{\cdot-}$ or $8^{\cdot-}$) have substantially lower activation energy for the fragmentation reaction than that corresponding to radical anions produced from **1** ($3^{\cdot-}$ or $4^{\cdot-}$), which favors the formation of disubstitution products from **2**. Radical anions $3^{\cdot-}$ and $4^{\cdot-}$ have a geometry in which the Cl_{meta} -C bond is relatively planar (see angle α , Table 2), while $7^{\cdot-}$ and $8^{\cdot-}$ present a Cl_{meta} -C bond with a distortion from the optimal sp^2 geometry, facilitating the *intra*-ET and thus, the fragmentation of $7^{\cdot-}$ and $8^{\cdot-}$.

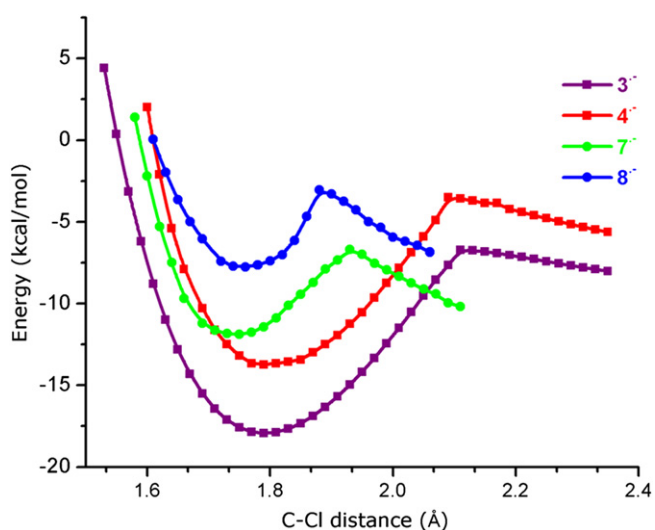


Fig. 3. UB3LYP/6-31+G* gas phase anionic profiles for fragmentation of methyl chlorobenzoate ($3^{\cdot-}$, violet), ($4^{\cdot-}$, red), ($7^{\cdot-}$, green), ($8^{\cdot-}$, blue). The neutral molecules were taken as zero energy.

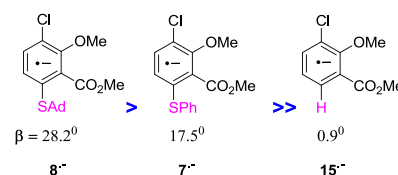
The topologies of the anionic PES depend on spin density, geometries and stability of substituted radical anions. Consequently, radical anions arising from **2** (blue or green) are more reactive, doing the formation of disubstitution product easier than that from **1**, in good agreement with the observed experimental behavior.

The formation of small amounts of **6** (Eq. 1) could also be explained on the basis of the stability of radical anions and the lower activation energy for the fragmentation process. This is so because the radical anions $4^{\cdot-}$ has a lower activation energy for the fragmentation process than the corresponding to radical anions $3^{\cdot-}$, explaining the formation of **6** (see Table 2).

The relative reactivity of both nucleophiles (PhS^- and AdS^-) with $11^{\cdot-}$ could be clarified considering the coupling reaction. In this reaction with AdS^- , the transition state has higher steric hindrance owing to the size of the adamantyl group, which retards the

coupling reaction. Thus, the coupling reaction of $11^{\cdot-}$ with PhS^- is faster than the corresponding with AdS^- as observed in this study.

Finally, for *meta*-chlorinated radical anions ($7^{\cdot-}$, $8^{\cdot-}$ and $15^{\cdot-}$), the reactivity could be interpreted in terms of the size of the substituent at *ortho*-position, which directly affects the rotation of the ester group (β dihedral angle) as follows:



Based on calculations, the spin densities and geometry of RAs, and the activation energies obtained for the fragmentation process reproduce the reactivity observed in the experimental conditions (see Supplementary data).

3. Conclusions

We report the synthesis of new compounds with potential herbicide activity. Syntheses were carried out by a $S_{RN}1$ reaction between either methyl 2,5-dichlorobenzoate (**1**) or methyl 3,6-dichloro 2-methoxybenzoate (**2**) with PhS^- or AdS^- in liquid NH_3 . Compound **1** afforded mainly the corresponding monosubstitution product, with retention of the chlorine, whereas **2** yielded the corresponding disubstitution product with both nucleophiles. The different reactivity observed, leading to the formation of either mono or disubstitution products, was explained on the basis of the activation energy necessary for the fragmentation of RAs. Changes in the general mechanism, as a consequence of a substituent have been not frequently observed in $S_{RN}1$ mechanism.

Additionally, the relative reactivity of PhS^- and AdS^- , with the radical formed by homolytic cleavage at *ortho*-position, with respect to the ester group from **1** or **2** ($11^{\cdot-}$) was clarified considering the steric hindrance caused by the adamantyl moiety.

The AdS^- ion has never been reported as a nucleophile to $S_{RN}1$ reactions. So far, our present results provide an excellent methodology to introduce the adamantyl group in bioactive molecules, which is very important for drug design.¹⁹

All in all, our current results present an interesting pathway for the production of new derivatives with potential herbicide activity. Furthermore, the combined use of experimental design with theoretical calculations, including evaluation of relative reactivity, provides with a powerful tool to design the synthesis of more derivatives using different substituents, which could help to produce environmentally friendly bioactive compounds.

4. Experimental section

4.1. Reagents

Dicamba, methyl 2,5-dichlorobenzoate, $PhSH$, $AdSH$, t -BuOK were commercially available and used as received. DMSO was distilled under vacuum and stored under molecular sieves (4 Å). Disugran was synthesized from Dicamba by esterification with IME in DMSO. Similarly, methyl 3-chloro-2-methoxybenzoate (**15**) was synthesized from 3-chloro-2-methoxybenzoic acid by esterification. Methyl 6-chloro-2-methoxybenzoate (**16**) was synthesized according to reported procedures²⁰ by halogen metal exchange (HME).

4.2. General methods

Irradiation was conducted in a reactor equipped with two 400-W UV lamps emitting maximally at 350 nm (Philips Model HPT, water-refrigerated).

4.2.1. Photostimulated reactions of methyl 2,5-dichlorobenzoate with PhS⁻ ions in liquid ammonia. The following procedure is representative of these reactions. PhSH (5 mmol) and *t*-BuOK (5.1 mmol) were added to 250 mL of distilled liquid ammonia; PhS⁻ ions were ready for use. The substrate, methyl 2,5-dichlorobenzoate (1 mmol), was added to the solution, and the reaction mixture was irradiated for 2 h. The reaction was then quenched with an excess of ammonium nitrate (or methyl iodide), and the ammonia was allowed to evaporate. The solid was dissolved in water, and HNO₃ was added to the water phase to reach pH=3 before extraction with diethyl ether. Products were isolated by column chromatography employing silica gel and quantified by GC using the internal standard method.

4.2.2. Dark reactions with PhS⁻ ions in liquid ammonia. This procedure was similar to that described for the previous reaction, except that the reaction flask was wrapped with aluminum foil.

4.2.3. Inhibited reactions using PhS⁻ ions in liquid ammonia. This procedure was similar to that described for the previous reaction, except that 30 mol % of *m*-DNB was added to the solution of the nucleophile prior to the addition of the substrate.

4.3. Isolation and characterization

4.3.1. Methyl 5-chloro-2-(phenylthio)benzoate (3). The product was purified as a colorless oil by column chromatography employing diethyl ether/petroleum ether (2:98) ¹H NMR (400 MHz, CDCl₃) δ: 3.96 (3H, s); 6.73 (1H, d, *J*=8.8 Hz); 7.19 (1H, dd, *J*=2.4, 8.7 Hz); 7.40–7.58 (5H, m); 7.96 (1H, d, *J*=2.4 Hz). ¹³C NMR (100 MHz, CDCl₃) δ: 52.5; 127.8; 128.7; 129.4; 129.9; 130.2; 130.7; 132.0; 132.3; 135.5; 142.0; 165.8. HRMS [MNa]⁺ exact mass calcd for C₁₄H₁₁ClO₂S: 301.0066, found: 301.0064.

4.3.2. Methyl 2-(1-adamantylthio)-5-chlorobenzoate (4). The product was purified as a white solid by column chromatography employing diethyl ether/petroleum ether (2:98). Mp: 59.0–59.7 °C. ¹H NMR (400 MHz, CDCl₃) δ: 1.55–2.05 (15H, m); 3.91 (3H, s); 7.36 (1H, dd, *J*=2.5, 8.3 Hz); 7.51 (1H, d, *J*=8.2 Hz); 7.56 (1H, d, *J*=2.5 Hz). ¹³C NMR (100 MHz, CDCl₃) δ: 30.1; 36.0; 43.7; 49.9; 52.5; 128.1; 128.6; 130.0; 134.8; 140.3; 141.0; 167.7. HRMS [MNa]⁺ exact mass calcd for C₁₈H₂₁ClO₂S: 359.3934, found: 359.3934.

4.3.3. Methyl 2,5-bis(1-adamantylthio)benzoate (6). The product was purified as a white solid by column chromatography employing diethyl ether/petroleum ether (2:98). Mp: 185.5–186.5 °C ¹H NMR (400 MHz, CDCl₃) δ: 1.54–2.08 (30H, m); 3.89 (3H, s); 7.49–7.58 (2H, m); 7.66 (1H, d, *J*=1.6 Hz). ¹³C NMR (100 MHz, CDCl₃) δ: 30.2; 30.3; 36.0; 43.6; 43.8; 48.7; 49.8; 52.1; 130.4; 131.7; 136.8; 138.5; 138.6; 139.6; 168.1. HRMS [MH]⁺ exact mass calcd for C₂₈H₃₆O₂S₂: 469.2229, found: 469.2233.

4.3.4. Methyl 2-methoxy-3,6-bis(phenylthio)benzoate (9). The product was purified as a yellow oil by column chromatography employing diethyl ether/petroleum ether (2:98). ¹H NMR (400 MHz, CDCl₃) δ: 3.91 (3H,s); 3.94 (3H,s); 6.83 (1H, d, *J*=8.5 Hz); 6.87 (1H, d, *J*=8.5 Hz); 7.24–7.43 (10H, m). ¹³C NMR (100 MHz, CDCl₃) δ: 52.6; 62.2; 127.7; 128.16; 128.2; 129.3; 129.6; 130.8; 131.0;

131.7; 131.9; 132.6; 132.9; 133.1; 134.6; 154.6; 166.8. HRMS [MH]⁺ exact mass calcd for C₂₁H₁₉O₃S₂: 383.0776, found: 383.0770.

4.3.5. Methyl 3,6-bis(1-adamantylthio)-2-methoxybenzoate (10). The product was purified as a white solid by column chromatography employing diethyl ether/petroleum ether (2:98). Mp: 188.5–190 °C ¹H NMR (400 MHz, CDCl₃) δ: 1.54–2.08 (30H, m); 3.92 (3H, s); 3.93 (3H, s); 7.23 (1H, d, *J*=8.1 Hz) 7.45 (1H, d, *J*=7.9 Hz). ¹³C NMR (100 MHz, CDCl₃) δ: 30.1; 30.15; 36.06; 36.1; 43.8; 43.9; 50.1; 50.4; 52.3; 63.0; 125.9; 130.5; 133.1; 136.9; 139.8; 159.4; 167.5. HRMS [MNa]⁺ exact mass calcd for C₂₉H₃₈O₃S₂: 521.2155, found: 521.2187.

4.3.6. Methyl 2-methoxy-6-(phenylthio)benzoate (17). The product was purified as yellow oil after chromatographic column employing petroleum ether (60:80). ¹H NMR (400 MHz, CDCl₃) δ: 3.84 (3H, s); 3.88 (3H, s); 6.80–6.87 (2H, m); 7.19–7.38 (6H, m). ¹³C NMR (100 MHz, CDCl₃) δ: 52.4; 56.1; 109.9; 124.4; 126.1; 127.4; 129.2; 130.8; 131.6; 134.8; 135.1; 156.7; 167.2. HRMS [MNa]⁺ exact mass calcd for C₁₅H₁₄O₃S: 297.0556 found: 297.0551.

4.4. Computational procedure

All calculations were carried out with DFT methods, as implemented in the Gaussian 03 package,¹⁵ by employing the B3LYP16²¹ functional at the 6-31+G* level of theory. This methodology is known to be appropriate for the theoretical study of the electronic and geometric properties of RAs.²² Stationary points were characterized by the normal analysis and obtained with complete geometry optimization without symmetry restrictions. Potential energy surfaces (PES) were obtained by varying the C_{meta}–Cl bond length. The transition state structures were optimized, characterized, and confirmed by IRC calculations. In all cases, the B3LYP spin contamination along the whole fragmentation path was negligible (*S*² = 0.750 – 0.751). For more details see [Supplementary data](#).

Supplementary data

Supplementary data related to this article can be found online at doi:10.1016/j.tet.2011.10.107.

References and notes

- (a) Rossi, R. A.; Pierini, A. B.; Peñeñory, A. B. *Chem. Rev.* **2003**, *103*, 71; (b) Rossi, R. A.; Peñeñory, A. B. The Photostimulated S_{RN}1 Process: Reaction of Haloarenes with Carbanions In *CRC Handbook of Organic Photochemistry and Photobiology*, 2nd ed.; Horspool, W. M., Lenel, F., Eds.; CRC: Boca Raton, USA, 2004, Chapter 47 pp 1–28; (c) Rossi, R. A. Photoinduced Aromatic Nucleophilic Substitution Reactions In *Synthetic Organic Photochemistry*; Griesbeck, A. G., Mattay, J., Eds.; Marcel Dekker: New York, NY, 2005; pp 495–527; (d) Rossi, R. A.; Pierini, A. B.; Santiago, A. N. In *Organic Reactions*; Paquette, L. A., Bittman, R., Eds.; Wiley: 1999; 54, pp 1–271.
- Bunnett, J. F.; Creary, X. J. *Org. Chem.* **1974**, *39*, 3173.
- Bunnett, J. F.; Creary, X. J. *Org. Chem.* **1975**, *40*, 3740.
- (a) Pierini, A. B.; Baumgartner, M. T.; Rossi, R. A. *J. Org. Chem.* **1991**, *56*, 580; (b) Baumgartner, M. T.; Pierini, A. B.; Rossi, R. A. *J. Org. Chem.* **1993**, *58*, 2593.
- (a) Beugelmans, R.; Chbani, M. *Bull. Soc. Chim. Fr.* **1995**, *132*, 290; (b) Beugelmans, R.; Bois-Choussy, M. *Tetrahedron* **1986**, *42*, 1381.
- (a) Pastor, S. D. *Helv. Chim. Acta* **1988**, *71*, 859; (b) Nasielski, J.; Moucheron, C.; Nasielski-Hinkens, R. *Bull. Soc. Chim. Belg.* **1992**, *101*, 491; (c) Singh, P.; Arora, G. *Tetrahedron* **1988**, *44*, 2625; (d) Baumgartner, C. D.; Malen, A. H.; Pastor, S. D.; NabiRahni, M. A. *Helv. Chim. Acta* **1992**, *75*, 480.
- (a) Bunnett, J. F.; Creary, X. J. *Org. Chem.* **1974**, *39*, 3611; (b) Amatore, C.; Beugelmans, R.; Bois-Choussy, M.; Combellas, C.; Thiébaud, A. *J. Org. Chem.* **1989**, *54*, 5688; (c) Novi, M.; Garbarino, G.; Petrillo, G.; Dell'Erba, C. *Tetrahedron* **1990**, *46*, 2205; (d) Petrillo, G.; Novi, M.; Garbarino, G.; Dell'Erba, C. *Tetrahedron* **1986**, *42*, 4007.
- Shaw, J. E. *J. Org. Chem.* **1991**, *56*, 3728.
- Palacios, S. M.; Alonso, R. A.; Rossi, R. A. *Tetrahedron* **1985**, *41*, 4147.
- Ahbalá, M.; Hapiot, P.; Houmam, A.; Jouini, M.; Pinson, J.; Saveant, J. M. *J. Am. Chem. Soc.* **1995**, *117*, 11488.
- Basso, S. M.; Montañez, J. P.; Santiago, A. N. *Lett. Org. Chem.* **2008**, *5*, 633.
- Montañez, J. P.; Uranga, J. G.; Santiago, A. N. *New J. Chem.* **2010**, *34*, 1170.

13. Bunnett, J. F. In *Investigation of Rates and Mechanisms of Reactions*, 3rd ed.; Lewis, E. S., Ed.; Wiley-Interscience: New York, NY, 1974; Part I, p 159.
14. The equation used in the relative reactivity determination of pairs of nucleophile was: $k_{\text{PhS}^-}/k_{\text{AdS}^-} = [\text{PhSAr}]_t [\text{AdS}^-]_0 / [\text{AdSAr}]_t [\text{PhS}^-]_0$, where $[\text{PhS}^-]_0$ and $[\text{AdS}^-]_0$ are initial concentrations and $[\text{PhSAr}]_t$ and $[\text{AdSAr}]_t$ are concentrations at time t of products, taking into account products 9, 10 and 14. This equation is based on a first-order reaction of both radical anions intermediates with nucleophiles.
15. Frisch, M. J., et al. *Gaussian 03*; Gaussian: Pittsburg, PA, 2003.
16. Pierini, A. B.; Duca, J. S.; Vera, D. M. A. *J. Chem. Soc., Perkin Trans. 2* **1999**, 1003 See also Ref. 12.
17. Pierini, A. B.; Vera, D. M. A. *J. Org. Chem.* **2003**, 68, 9191.
18. (a) Heinis, T.; Chowdhury, S.; Scott, S. L.; Kebarle, P. *J. Am. Chem. Soc.* **1987**, 110, 400; (b) Kebarle, P.; Chowdhury, S. *Chem. Rev.* **1987**, 87, 513.
19. Liu, J.; Obando, D.; Liao, V.; Lifa, T.; Codd, R. *Eur. J. Med. Chem.* **2011**, 46, 1949.
20. Santiago, A. N.; Basso, S. M.; Montañez, J. P.; Rossi, R. A. *J. Phys. Org. Chem.* **2006**, 19, 829.
21. (a) Lee, C.; Yang, W.; Parr, R. G. *Phys. Rev. B* **1988**, 37, 785; (b) Becke, A. D. *Phys. Rev. A* **1988**, 38, 3098; (c) Miehlich, B.; Savin, A.; Stoll, H.; Preuss, H. *Chem. Phys. Lett.* **1989**, 157, 200.
22. (a) Vera, D. M. A.; Pierini, A. B. *Phys. Chem. Chem. Phys.* **2004**, 6, 2899; (b) Uranga, J. G.; Vera, D. M. A.; Santiago, A. N.; Pierini, A. B. *J. Org. Chem.* **2006**, 71, 6596; (c) Uranga, J. G.; Santiago, A. N. *New J. Chem.* **2010**, 34, 2006; (d) Uranga, J. G.; Santiago, A. N. *Org. Biomol. Chem.* **2011**, 9, 2669.